

## Supplemental Material

### Data compilation and filtering

All basaltic samples were compiled from literature, and all of them are geographically distributed in the east of the North-South Gravity Lineation (Fig. 3A). We only included samples younger than 200 Ma because older mafic samples are scarce (Zhang et al., 2014), and cannot provide meaningful records on lithospheric thickness. The rock types mainly include basalt, alkaline basalt, lamprophyre, basanite, and nephelinolite. To avoid post-magmatic alteration, we exclude samples of LOI >4wt.% and re-normalize major oxide components to 100 wt.% on a volatile-free basis. Because the compositions of evolved magmas cannot be effectively corrected for fractionation, we only included samples with SiO<sub>2</sub> <55 wt.%, MgO >7.5wt.%, whose differentiation is primarily controlled by olivine fractionation (Herzberg, 2006). We also excluded samples with  $Eu/Eu^* > 1.1$  (chondrite normalized  $Eu/\sqrt{(Sm \times Gd)}$  ) to eliminate crystal-rich cumulates. For samples calculated using the geobarometer from Sun and Dasgupta, we screened out samples with silica-alumina index  $\leq 0$  (i.e.,  $SAI = SiO_2 + 2/3Al_2O_3 - TiO_2 - 2(Na_2O + K_2O) - 50$ , oxides are expressed as molar percentages on a volatile-free basis). After these filtering procedures, the number of remaining samples was reduced to 339.

### Geobarometers and equilibrium pressure calculation

The two geobarometers developed by Lee et al., and Sun and Dasgupta were designed to calculate pressure for different types of basaltic melts. The geobarometer calibrated by

Lee et al. can only be applied to melts equilibrated with peridotites, and is most suitable for spinel-peridotite melts because the  $\text{SiO}_2$  content of garnet-peridotite melts is much less pressure-sensitive than those of spinel-peridotite melts. In addition, this geobarometer was calibrated for  $\text{CO}_2$ -free systems and thus should not be applied to  $\text{CO}_2$ -rich mafic magmas. The second geobarometer calibrated by Sun and Dasgupta requires the existence of garnet in the source to buffer melt  $\text{Al}_2\text{O}_3$  content and is applicable for  $\text{CO}_2$ -rich, silica-undersaturated melts. The uncertainties of these two geobarometers are 0.4 GPa and 1.0 GPa at the  $2\sigma$  level of confidence, respectively.

In the North China Craton, mafic magmas  $< \sim 120$  Ma were likely derived from mantle rocks contaminated by subducted carbonates because they have systematically low  $\delta^{26}\text{Mg}$  relative to that of normal mantle (Fig. S1; Li et al., 2017; Yang et al., 2012). Therefore, for all samples younger than 120 Ma, we used the geobarometer calibrated by Sun and Dasgupta to calculate their equilibrium pressures. Because pyroxenite source lacks olivine, the equilibrium pressures of potential pyroxenite-sourced samples ( $\text{Fe}/\text{Mn} > 60$ ; Fig. S2) were calculated using the geobarometer from Sun and Dasgupta. The remaining samples, whose sources consist of peridotite, were subdivided into two groups based on the  $\text{SiO}_2$  content. Samples with  $\text{SiO}_2 \geq 50$  wt.% were calculated by using the geobarometer from Lee et al., whereas the equilibrium pressures for samples with  $\text{SiO}_2 < 50$  wt.% were calculated using the geobarometer from Sun and Dasgupta.

Before applying the geobarometers, one needs to correct for fractionation to obtain primary magma compositions. There are three critical parameters that affect the calculation of primary magma compositions: oxygen fugacity (expressed as  $\text{Fe}^{3+}/\text{Fe}_T$ ),  $\text{Fe}^{2+}$ -Mg exchange coefficient between olivine and melt (i.e.,  $K_D = (\text{Fe}^{2+}/\text{Mg})_{\text{ol}}/(\text{Fe}^{2+}/\text{Mg})_{\text{melt}}$ ), and mantle source composition.  $\text{Fe}^{3+}/\text{Fe}_T$  and  $K_D$  were assumed to be 0.1 and 0.32, respectively (Herzberg and Asimow, 2008; Roeder and Emslie, 1970). We determined the mantle olivine Fo (i.e., the mole fraction of  $\text{Mg}_2\text{SiO}_4$  in olivine) based on peridotite xenoliths from North China Craton. Early Cretaceous magma entrained peridotite xenoliths mostly have Fo value of 92 (Liu et al., 2011; Xu et al., 2010), which is the typical value for refractory Archean cratonic peridotite (Griffin et al., 2003). Therefore, we set the mantle source Fo value at 92 for  $\geq 120$  Ma samples, whose Nd isotopic signatures indicate intense interaction with the lithospheric mantle. Mantle peridotite xenoliths hosted by  $<120$  Ma basalts from the North China Craton have average olivine Fo of 89 (Xu et al., 2013; Zhao et al., 2012). Cenozoic peridotites with extremely low olivine Fo (e.g.,  $<85$ ) have also been discovered and were thought to have formed by interactions with carbonate-rich silicate melts (Xiao et al., 2010). Based on these findings, we set the mantle Fo value to be 89 for samples  $<120$  Ma (Fig. 2B). Lower mantle olivine Fo values will lead to lower calculated equilibrium pressures for the Cenozoic basalts (Fig. S3). Another concern relates to pyroxenite-sourced melts. Mantle pyroxenites generally form from metasomatism, and pyroxenite sourced melts are more evolved (Sobolev et al., 2005). Therefore, using peridotite olivine Fo may lead to

overcorrections of fractionation and overestimates of equilibrium pressures for pyroxenite-sourced melts. Many of the mafic rocks from the North China Craton show Fe/Mn ratios >60 (Fig. S2), a sign of contributions from pyroxenite-sourced melts (Herzberg, 2011). For these samples, our calculation yielded the upper bounds on their equilibrium pressures.

### **Surface subsidence/uplift calculations**

Surface subsidence/uplift (s) was calculated as the difference between the actual elevation and that predicted from the Airy isostasy principle:

$$s = h - [(1 - \rho_{cc}/\rho_m) * H_{cc} + (\rho_{oc}/\rho_m - 1) * H_{oc} + (\rho_{ow}/\rho_m - 1) * H_{ow}], \quad (1)$$

where  $h$  is the actual elevation,  $H_{cc}$  is the thickness of the continental crust,  $H_{oc}$  is the thickness of the oceanic crust,  $H_{ow}$  is the average oceanic water depth,  $\rho_{cc}$  is the density of the continental crust,  $\rho_{oc}$  is the density of the oceanic crust,  $\rho_m$  is the density of the asthenospheric mantle, and  $\rho_{ow}$  is the density of the oceanic water. In this calculation, we adopted density values of 3.0 g/cm<sup>3</sup>, 3.3 g/cm<sup>3</sup>, and 1.0 g/cm<sup>3</sup> for the oceanic crust, asthenospheric mantle, and oceanic water. The thickness of the oceanic crust was set to be 7 km, and the average oceanic water depth to be 4 km. Crustal density values at different depth intervals along profiles aa', bb', and cc' in Fig. 3 were obtained from Deng and Levandowski, 2018. The actual elevation data along the same profiles were taken from Wei et al., 2016; Xu et al., 2016; Zhang et al., 2014. The exact value of the predicted elevation and thus surface subsidence are affected by the uncertainties of the

density of the mantle, the density of the oceanic crust, the thickness of the oceanic crust, and the average oceanic water depth. But these uncertainties would not change the systematic decreasing trends of surface subsidence/uplifting along profiles aa', bb', and cc' (Fig. 3B).

## REFERENCES

- Deng, Y., and Levandowski, W., 2018, Lithospheric Alteration, Intraplate Crustal Deformation, and Topography in Eastern China: *Tectonics*, v. 37, no. 11, p. 4120-4134.
- Griffin, W. L., O'Reilly, S. Y., Abe, N., Aulbach, S., Davies, R. M., Pearson, N. J., Doyle, B. J., and Kivi, K., 2003, The origin and evolution of Archean lithospheric mantle: *Precambrian Research*, v. 127, no. 1-3, p. 19-41.
- Herzberg, C., 2006, Petrology and thermal structure of the Hawaiian plume from Mauna Kea volcano: *Nature*, v. 444, no. 7119, p. 605-609.
- Herzberg, C., 2011, Identification of Source Lithology in the Hawaiian and Canary Islands: Implications for Origins: *Journal of Petrology*, v. 52, no. 1, p. 113-146.
- Herzberg, C., and Asimow, P. D., 2008, Petrology of some oceanic island basalts: PRIMELT2. XLS software for primary magma calculation: *Geochemistry, Geophysics, Geosystems*, v. 9, no. 9.
- Lee, C.-T. A., Luffi, P., Plank, T., Dalton, H., and Leeman, W. P., 2009, Constraints on the depths and temperatures of basaltic magma generation on Earth and other terrestrial planets using new thermobarometers for mafic magmas: *Earth and Planetary Science Letters*, v. 279, no. 1-2, p. 20-33.
- Li, S.-G., Yang, W., Ke, S., Meng, X., Tian, H., Xu, L., He, Y., Huang, J., Wang, X.-C., Xia, Q., Sun, W., Yang, X., Ren, Z.-Y., Wei, H., Liu, Y., Meng, F., and Yan, J., 2017, Deep carbon cycles constrained by a large-scale mantle Mg isotope anomaly in

- eastern China: *National Science Review*, v. 4, no. 1, p. 111-120.
- Liu, J., Rudnick, R. L., Walker, R. J., Gao, S., Wu, F.-y., Piccoli, P. M., Yuan, H., Xu, W.-l., and Xu, Y.-G., 2011, Mapping lithospheric boundaries using Os isotopes of mantle xenoliths: An example from the North China Craton: *Geochimica et Cosmochimica Acta*, v. 75, no. 13, p. 3881-3902.
- Roeder, P., and Emslie, R., 1970, Olivine-liquid equilibrium: Contributions to mineralogy and petrology, v. 29, no. 4, p. 275-289.
- Sun, C., and Dasgupta, R., 2020, Thermobarometry of CO<sub>2</sub>-rich, silica-undersaturated melts constrains cratonic lithosphere thinning through time in areas of kimberlitic magmatism: *Earth and Planetary Science Letters*, v. 550.
- Sobolev, A. V., Hofmann, A. W., Sobolev, S. V., and Nikogosian, I. K., 2005, An olivine-free mantle source of Hawaiian shield basalts: *Nature*, v. 434, no. 7033, p. 590-597.
- Wei, Z., Chen, L., Li, Z., Ling, Y., and Li, J., 2016, Regional variation in Moho depth and Poisson's ratio beneath eastern China and its tectonic implications: *Journal of Asian Earth Sciences*, v. 115, p. 308-320.
- Xiao, Y., Zhang, H.-F., Fan, W.-M., Ying, J.-F., Zhang, J., Zhao, X.-M., and Su, B.-X., 2010, Evolution of lithospheric mantle beneath the Tan-Lu fault zone, eastern North China Craton: Evidence from petrology and geochemistry of peridotite xenoliths: *Lithos*, v. 117, no. 1-4, p. 229-246.
- Xu, R., Liu, Y., Tong, X., Hu, Z., Zong, K., and Gao, S., 2013, In-situ trace elements

- and Li and Sr isotopes in peridotite xenoliths from Kuandian, North China Craton: Insights into Pacific slab subduction-related mantle modification: *Chemical Geology*, v. 354, p. 107-123.
- Xu, W., Yang, D., Gao, S., Pei, F., and Yu, Y., 2010, Geochemistry of peridotite xenoliths in Early Cretaceous high-Mg# diorites from the Central Orogenic Block of the North China Craton: The nature of Mesozoic lithospheric mantle and constraints on lithospheric thinning: *Chemical Geology*, v. 270, no. 1-4, p. 257-273.
- Xu, Y., Zeyen, H., Hao, T., Santosh, M., Li, Z., Huang, S., and Xing, J., 2016, Lithospheric structure of the North China Craton: Integrated gravity, geoid and topography data: *Gondwana Research*, v. 34, p. 315-323.
- Yang, W., Teng, F.-Z., Zhang, H.-F., and Li, S.-G., 2012, Magnesium isotopic systematics of continental basalts from the North China craton: Implications for tracing subducted carbonate in the mantle: *Chemical Geology*, v. 328, p. 185-194.
- Zhang, Z., Zhang, G., Deng, Y., Santosh, M., and Teng, J., 2014, Geophysical transect across the North China Craton: A perspective on the interaction between Tibetan eastward escape and Pacific westward flow: *Gondwana Research*, v. 26, no. 1, p. 311-322.
- Zhao, X., Zhang, H., Zhu, X., Tang, S., and Yan, B., 2012, Iron isotope evidence for multistage melt–peridotite interactions in the lithospheric mantle of eastern China: *Chemical Geology*, v. 292-293, p. 127-139.
- Zhu, R., Xu, Y., Zhu, G., Zhang, H., Xia, Q., and Zheng, T., 2012, Destruction of the



North China craton: Science China Earth Sciences, v. 55, no. 10, p. 1565-1587.

Figure S1. Plot of  $\delta^{26}\text{Mg}$  versus age (Ma) for the mafic magmas from eastern China.

Samples with age <120 Ma show Mg isotopic compositions deviate from normal mantle value, which are indicative of subducted carbonate in their source mantle.

Figure S2. Plot of Fe/Mn versus age (Ma) for samples used in calculations. Peridotite-derived melts have  $\text{Fe/Mn} \leq 60$ , whereas that of pyroxenite or eclogite have  $\text{Fe/Mn} > 60$  (Herzberg, 2011). We use Fe/Mn ratios of mantle-derived mafic magmas to differentiate mantle sources and to decide which geobarometer can be applied.

Figure S3. Test of the effect of mantle olivine Fo on the calculated pressures for mafic magmas. In (A), (B), and (C), we adopted  $\text{Fo} = 92$  for magmas with age  $\geq 110$  Ma and for age <110 Ma magmas, the mantle olivine Fo was assumed to be 88, 86, and 84, respectively. Lowering the Fo value would reduce the pressures recorded by these mafic magmas.

Figure S4. Plot of  $(\text{La/Yb})_{\text{N}}$  ratios versus age (Ma) for magmas used in calculations. The  $(\text{La/Yb})_{\text{N}}$  shows sharp decrease at 130-120Ma, broadly consistent with the calculated pressures.

Figure S1

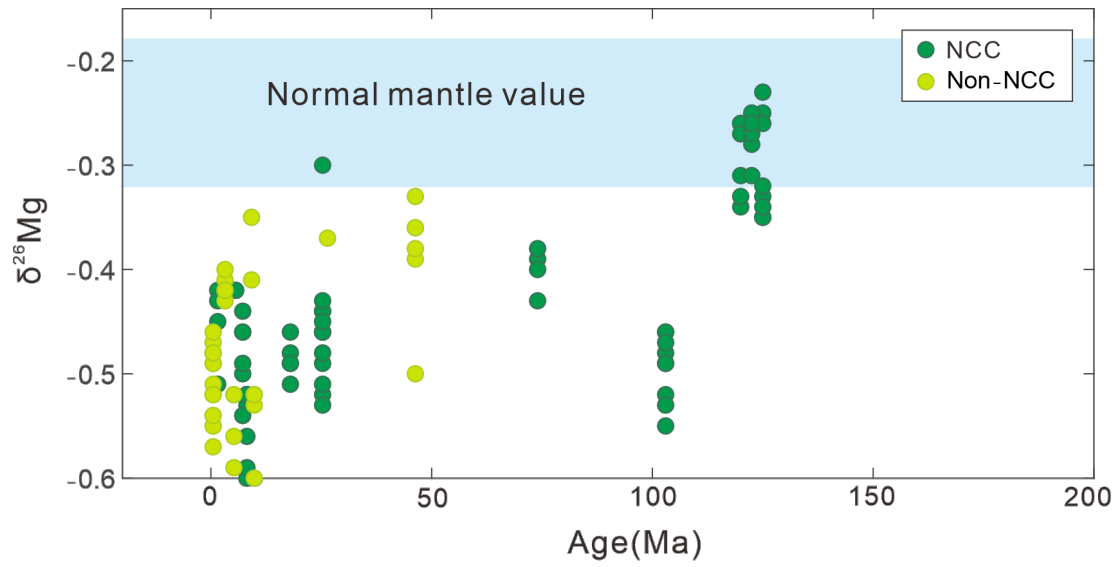


Figure S2

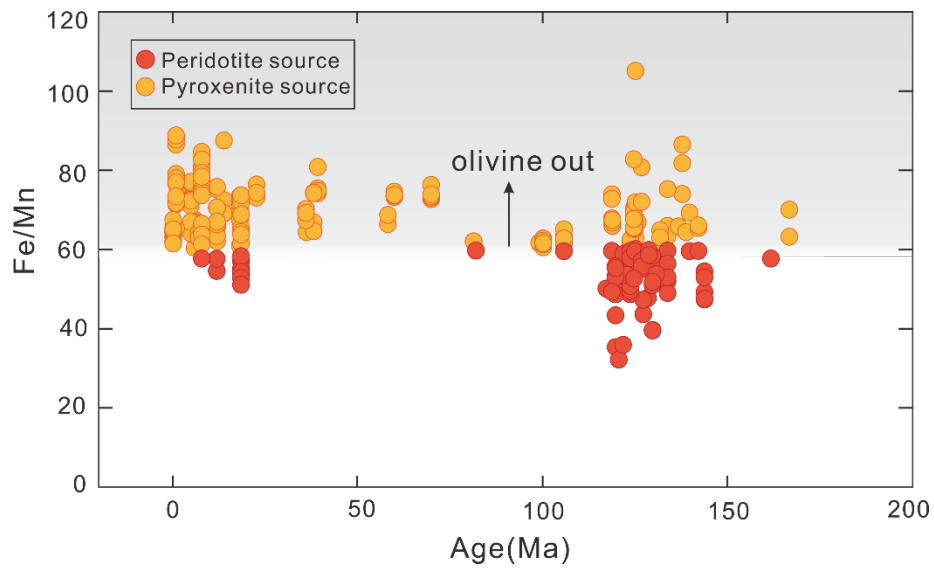


Figure S3

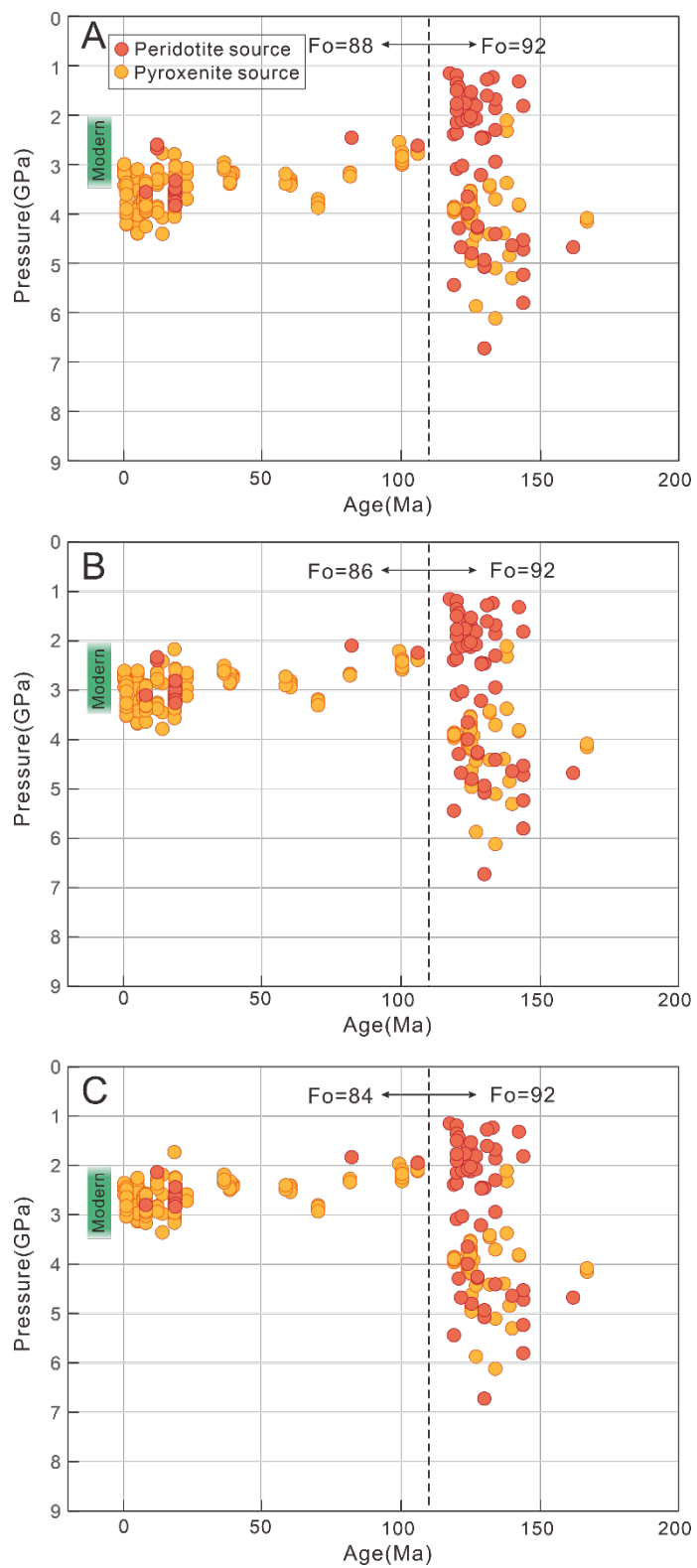


Figure S4

